FLYEYE TELESCOPE 2.0 STUDY

Piero Gregori[(1)], Roberta Pellegrini[(2)], Andrea Guazzora[(3)], Silvano Pieri[(4)], Francesco Cerutti[(5)], Luca Orioli[(6)], Ernesto Doelling[(7)], Bernd Sierk[(8)], Robert Daddato[(9)], Luca Conversi[(10)]

(1) OHB-Italia, Via Gallarate 150, 20151 Milan (MI), Italy, Email: piero.gregori@ohb-italia.it
(2) OHB-Italia, Via Gallarate 150, 20151 Milan (MI), Italy, Email: roberta.pellegrini@ohb-italia.it
(3) OHB-Italia, Via Gallarate 150, 20151 Milan (MI), Italy, Email: andrea.guazzora@ohb-italia.it
(4) OHB-Italia, Via Gallarate 150, 20151 Milan (MI), Italy, Email: silvano.pieri.ext@ohb-italia.it
(5) OHB-Italia, Via Gallarate 150, 20151 Milan (MI), Italy, Email: francesco.cerutti@ohb-italia.it
(6) OHB-Italia, Via Gallarate 150, 20151 Milan (MI), Italy, Email: luca.orioli@ohb-italia.it
(7) European Space Agency, Robert-Bosch-Str. 5 – 64293 Darmstadt, Germany, Email: ernesto.doelling@esa.int
(8) European Space Agency, Robert-Bosch-Str. 5 – 64293 Darmstadt, Germany, Email: Bernd.Sierk@esa.int
(9) European Space Agency, Robert-Bosch-Str. 5 – 64293 Darmstadt, Germany, Email: Robert.Daddato@esa.int
(10) European Space Agency, Robert-Bosch-Str. 5 – 64293 Darmstadt, Germany, Email: Luca.Conversi@esa.int

ABSTRACT

ESA's Flyeye Telescope prototype, developed in the frame of the NEOSTED (NEO Survey Telescope Deployment) ESA program, has revealed some limitations to achieve the limiting magnitude over its wide field of view (FoV). This study is mainly focused on developing an upgraded Flyeye telescope capable of detecting asteroids down to V magnitude of 21.0 with a minimum peak SNR of 5.0 over at least the 95% of the entire Field of View.

Newer modifications and upgrades are considered, such as the reduction of the optical central obstruction, the number and the design of the optical channels. A preliminary performance analysis, based on the SNR model, is performed in order to confirm the quality of the improvements of the new optical design.

1. BACKROUND

The Flyeye concept was born from an intuition of Prof. Roberto Ragazzoni to monitor the large number of orbiting objects, the residue of decades of tumultuous space activity, as well as the more traditional asteroids.

For this type of monitoring, a rapid reconnaissance of the entire celestial vault is crucial, in order to discover bodies with dangerous trajectories, with sufficient advance for in-depth analysis and/or defensive interventions.

In optical astronomy, the instrument which is typically characterized by a large field of view is the Schmidt telescope. The Flyeye concept represents its evolution.

The essential elements of the Flyeye are:

- A spherical primary mirror (PM) as the common collector of the entire field of view
- A specular optical group, called Beam Shaper (BS), placed near the primary focus, with the task of splitting the field of view into multiple distinct optical channels
- A series of equal Secondary Optical Tubes (SOT), one for each channel, which create secondary images of the respective portions of the field in separate CCD cameras. On each channel, near the BS, there is a field lens to correct the exit pupil image.

The optical axes of all channels pass through the centre of curvature of the primary mirror as happens in the Schmidt telescope. Unlike this, however, there is not any aspherical plate on the mirror centre of curvature. The correction of the spherical aberration of the primary mirror and of the field curvature is made channel by channel by the SOT and by the associated field lens.

The shape of the BS is the crucial element of the concept. Seen from the direction of the telescope axis, the BS must appear as a regular mosaic, in which each face is a flat mirror intercepting a portion of the field. the orientation of each face must be such as to direct, together with all the others, the optical axes of the associated channels according to an appropriately distributed sunburst.

Due to their inclination, the faces intercept the optical beam with variable defocus with respect to their contour. This defocus, near the edges, causes a growing vignetting along the border sides between them. This 'transitional' vignetting V_t is well known and is intrinsic to the Flyeye concept. The correct design of the slopes must ensure that its extension is minimal. $V_t = 1$ in the central area of the field, where the face intercepts the entire beam.

However, there is also a positive effect. Vignetting creates a 'fading' transition from one piece of the field to its adjacent, without gaps, but only with a reduced illuminance.

Proc. 2nd NEO and Debris Detection Conference, Darmstadt, Germany, 24-26 January 2023, published by the ESA Space Safety Programme Office
Ed. T. Flohrer, R. Moissl, F. Schmitz (http://conference.sdo.esoc.esa.int, February 2023)

2. NEOSTEL DEVELOPMENT

The first Flyeye application was the Near-Earth Object Survey Telescope (NEOSTEL), as the core Optical Sensor of the NEO-S2P Segment Ground Based Optical Observation Network. The scientific requirements were mainly focused on the Survey and Tracking of Near-Earth Objects (NEOs).

The telescope shall be capable of conducing a wide survey strategy, which consists in scanning the half of the night visible sky at least 4 times per night to detect NEO objects characterized by apparent magnitudes down to 21.5. NEOSTEL shall also allow the detection of fast approaching NEO objects, moving at apparent speeds up to 5 arcsec/min. NEOSTEL shall also be able to perform all required follow up activities, necessary for catalogue maintenance upgrading, impact monitoring, alert and mitigation, etc.

The aim of targeting objects at above mentioned magnitude while scanning half of the night visible sky at least 4 times per night, requires a one meter class aperture together with a very large FoV (> 44 sq. deg) and exposure times in the order of 40 s.

The above reported requirements are realized in the Flyeye architecture resulting in fast (EFL = 2000mm, i.e., F/# < 2) and seeing limited Optics ensuring an 80% Encircled Energy enclosed in <1" radius at 1.5" pixel scale. Starting from a 16 megapixel CCD sensor with a pixel size of 15 µm, the goal is achieved with 16 channels.

During the development of the first NEOSTED prototype, problems and difficulties arose, which escaped the design phase, relating to higher-than-expected vignetting and alignment difficulties. To some extent, they have been addressed and resolved with the remaking of some parts and with a new generation of alignment aids.

All these activities have allowed us to develop considerable experience on the Flyeye concept. Experience that we have poured into the study of the Flyeye Telescope 2.0.

3. FLYEYE 2.0 REQUIREMENTS AND NEWER DESIGN KEY POINTS

The requirements of Flyeye 2.0 are targeted to a specific operating environment and accentuate the attention on the SNR over the whole FoV. In particular, the following characteristics are highlighted:

A. Reference median seeing 1.5 arcsec FWHM
B. PSF FWHM sampling ratio between 1.6 and 2.4
C. Peak SNR of 5 down to V magnitude of 21.0, over at least 95% of the entire FOV.
D. 4 or more observations of every field separated by a TBD interval

The requirement B. refers to the overall PSF on the focal plane, including the contribution of seeing. This is the requirement that most clearly differentiates the new generation of Flyeye from the original prototype. Directly comparing this data alone, the NEOSTEL would have a ratio of 1.08.

The most relevant consequences of the necessary variants are:

- Increase focal length or decrease pixel size
- Reduction of EnsQuared Energy (EQE) in the pixel

To identify the necessary modification actions, we see in Table 1 the application of the sampling requirement to NEOSTEL design by reducing the pixel size.

Table 1: PSF Sampling vs Pixel EQE and Peak SNR

	Pixel size (µm)	Sampling	EQE	F_{eq} (m)	Peak SNR
NEOSTEL DESIGN	15	1.08	0.42	2.00	11.3
NEOSTEL DESIGN 1.6 Sampling	10	1.62	0.25	3.00	7.0
NEOSTEL DESIGN 2.0 Sampling	8	2.02	0.17	3.75	4.8

Alternatively, assuming that the contribution of optical aberration is kept proportional to the seeing contribution, on the PSF convolution, the focal length can be increased instead of reducing the pixel size (F_{eq} column). In either case, one must compensate for the reduction in EQE by increasing the area (A) of the entrance pupil.

The peak SNR column shows the maximum SNR value (central field) calculated with the radiometric model (eq. 1 below), applying the Flyeye 2.0 requirements to the NEOSTEL telescope.

In the radiometric model, the energy collected in the pixel is proportional to the product EQE * A * V_t. Therefore, wanting to restore the same SNR of line 1, in lines 2 and 3, A should be increased in proportion to the reduction of EQE.

The increment of the entrance pupil area A depends on multiple factors related to requirement C. Compared to NEOSTEL, this is a new requirement asking for the visual magnitude to be reduced from 21.5 to 21.0, ensuring the SNR>5 with 95% probability across the entire field of view.

To compensate for the presence of vignetting along the Field of View it is necessary that the SNR peak value is adequately greater than the threshold value.

The EQE values of Table 1, and thus also the required values of A, depend almost exclusively on the sampling. This is because the shape of the convoluted PSF is mainly determined by the seeing distribution.

Instead, the peak SNR margin that may be necessary depends on the degree of optimization of the BS faces orientation and, above all, on the number of transitions, i.e., on the number of channels.

4. NEW DESIGN TELESCOPE TRADEOFF

The possible solution for the Flyeye 2.0 is the result of the trade-off between these multiple parameters:

- Focal length vs pixel size.
- Number of channels vs channel field of view.
- Number of channels vs transition vignetting

With the same pupil area, reducing the focal length decreases the relative aperture and therefore, potentially increasing the contribution of optical aberration. This is a vicious circle because it increases the PSF FWHM, requiring you to reduce the focal length even further.

The number of channels has a great influence on the number of transitions between field tiles and therefore, on the field area subject to vignetting. On the other hand, with the same total field, the faces of the BS increase in size, with a consequent possible increase in the width of the individual transition zones. This consequence is not automatic. It can be expected that if there are fewer channels to distribute around the axis of the telescope it will be easier to optimize its inclinations.

Reducing the number of channels, however, also increases the field of view of each of them. This makes the design of the SOT more difficult, which will also be more voluminous and requires the availability of a camera with a different sensor.

The negative consequences of reducing the number of channels can be mitigated by accepting a reduction of the total field of view. This possibility is left open by the TBD present in requirement D.

5. THE SELECTED NEW DESIGN

The development of the telescope design covered a REDUCED CHANNELS concept design and an improvement of the 16 channels NEOSTED telescope. The reduced channels design is an 8 channels telescope with an overall field of view narrower than the 16 channels design but with a single channel field of view wider than the equivalent one in the 16 channels telescope. The improved 16 channels telescope has reduced the primary vignetting, transition vignetting and central obscuration respect to the first NEOSTED optical layout. The main monitor of the performance evaluation of both the design is the SNR, which is modelled by the following formula:

$$SNR = \frac{I \cdot T_h \cdot t \cdot EE}{\sqrt{(B)\, t + (C)}} \qquad (1)$$

where :

$I = I_0 \cdot 10^{-0.4V}$ ($phot/(s*m^2)$) is the flux density of the star as a function of the magnitude V;

I_0 ($phot/(s*m^2)$) is the flux density of a NEO of 0 magnitude, in the band of the telescope;

$T_h = A \cdot \tau \cdot \alpha$ ($m^2*e^-/phot$) is the overall throughput of the optical system that depends on:

- A (m^2) is the useful area of the entrance pupil;
- τ ($e^-/phot$) is the system peak efficiency. It is composed of two factors: transparency (tr) of the optical system through materials and coatings, and peak of the filtered Quantum Efficiency (QE ($e^-/phot$));
- α is the vignetting factor that depends on the location of the telescope's field-of-view point;

t is the exposition time (sec);

EE is the fraction of the whole PSF energy falling into the pixel;

$B = I \cdot T_h \cdot EE + I_{sky} \cdot T_h \cdot PS^2 + N_t$;

$C = RN^2 + G^2/4$

The parameter B depends also on T_h , on I_{sky} which is the flux density from the background, indeed a function of the corresponding magnitude V_{sky} ($MAG/arcsec^2$), on the pixel scale, on the temporal noise of the detector.

The parameter C depends on the sensor readout noise and on the sensor gain.

Table 2: Design trade off evaluation parameters

	Focal length [m]	F/#	Sampling	FoV [square degrees]	Peak SNR
16 CHANNELS / 15 um 36 Mp	2.75	2.39	1.7	49.80	10.1
16 CHANNELS / 10 um 81 Mp	2.15	2.01	1.8	37.94	8.3
8 CHANNELS / 15 um 36 Mp	2.60	2.56	1.6	26.86	8.0
8 CHANNELS / 10 um 81 Mp	2.30	2.15	2.1	37.11	5.3

The final evaluation has been done over two variants of both 8 channels and 16 channels designs, each variant closely depending on the pixel size to be chosen. The two feasible options are 10 µm and 15 µm pixel sizes, being

the feasibility based on the availability of these physical dimensions on the market. The dimension of the CCD sensor has been kept constant along the different telescope options, to fit a 36 Mpixels / 15 µm pixel size camera, and to save an 81 Mpixels / 10 µm pixel size camera as an option. Table 2 summarizes the main features and performances of the four evaluated design.

The transitions are the boundary regions between two or more channels. In these regions a fading effect of the signal appears, lowering the signal of a variable amount. What is relevant to obtain an effect on the SNR is the channel vignetting, which depends on the number of transitions per channel. The effective reduction is from 24/16 = 1.5 transitions to 10/8 = 1.25 transitions, per each telescope channel. The typical distribution of the cumulative telescope vignetting along the Field of View has its minimum on the optical axis, the centre of the considered sub-FoV as well. This causes the peak of the SNR to fall on axis too, and a lowering of the SNR off axis. Because the detection capability of the telescope depends inversely from the vignetting, a profitable design strategy to ensure the coverage of V-mag = 21 detection along the FoV is to have additional SNR margin on axis, with respect to the target peak value from the requirements. The margin of 3 points of SNR on axis, with respect to the value of 5 as from the requirement C, combined with the reduction of the transition vignetting, ensures the 95% field coverage of V-mag = 21 more easily than any other telescope design. For this reason, the 8 channels / 15 µm pixel size and 36 Mpixel camera has been selected as the newer Flyeye 2.0 telescope to be developed.

6. CONCISE ANALYSIS SUMMARY AND REDUCED CHANNELS TELESCOPE DESCRIPTION

The final evolution of the 8 channels telescope design started from the state of the project as depicted in Table 2. To develop the 8 channels telescope design until an optimum level of maturity, the design approach has been structured by two sequential models: the aberration free model and the real telescope model.

The aberration free model is the basic theoretical model needed to define the fundamental relations between the driving physical quantities of the project. The real telescope model is the optical design of the real telescope as a result of a design process. Starting from a first design built upon the basic rules of the aberration free model, the optical aberration has been added, and the final design has been derived by a trial and error design optimization.

As a summary of the basic rules which drive the aberration free model, we hereby declare the two equations describing the direct relations between the focal length and the pixel size (2), and between EE and sampling (3):

$$F_t = p_x \frac{s}{\Sigma} \tag{2}$$

$$EE = k_m \frac{PS^2}{\sigma^2} = \frac{k_m}{s^2} \tag{3}$$

where:

F_t is telescope focal length;

p_x is the pixel size;

s is the sampling;

$\Sigma = \sigma/3600 \cdot \frac{\pi}{180}$ is the seeing FWHM;

σ = angular FWHM;

k_m = Moffat seeing model constant among the limited domain of this application.

Proceeding by design key points, a quick summary of the design activity is listed hereinafter.

In the aberration free model the focal length is a direct function of the pixel size, and the Ensquared Energy is an inverse function of the squared sampling.

In the real telescope design the presence of the optical aberration determines a trade off between the minimum pixel size and the maximum Ensquared Energy.

The optimum balance is reached by optimizing the entrance pupil area A and the focal length F_t in a trial and error design process.

The main advances of the final telescope design are described here below.

The halving of the number of the optical channels moving from a 16 channels to an 8 channels design will heavily simplify the manufacturing and alignment, more easily fulfilling the target performances. The alignment tools are currently under revision: the change in focal length can imply some modifications in the optical tools used for alignment. This activity will surely be the occasion to try gaining an even more accurate telescope alignment.

The primary mirror of the Flyeye 2.0 is increased to a 1520 mm mechanical diameter, granting an optical surface diameter of 1460 mm. The radius of curvature is also increased to 4 m and the back side of the mirror is drilled in triangular flat pockets, thus reducing the weight by 55%. The off-loading system also changes from the NEOSTED astatic levers system to a whiffle-tree system. This solution allows to transfer the actuation system at PMC level: for NEOSTED the tripod motors were

directly interfaced to the primary mirror, now it is the whole cradle plus primary mirror system that is tip-tilted or pistoned. This new architecture allows in principle a maximum axial stroke of ±7.5 mm (Figure 1).

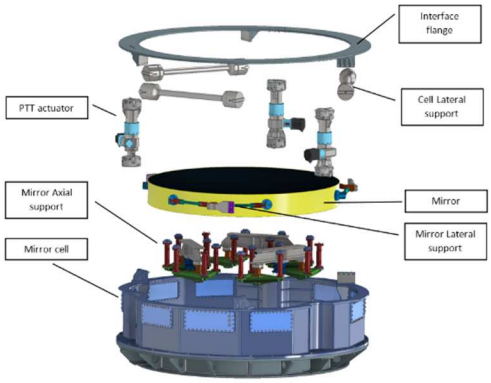

Figure 1: Primary Mirror and Cradle

The focusing capability is redesigned and moved from the current implementation at SOT level to a new implementation at camera level. This implementation ensures an improved sensitivity and effectiveness of the focusing adjustment. The focusing stroke could be very large to compensate all the possible needs (preliminary design stroke: ±3 mm).

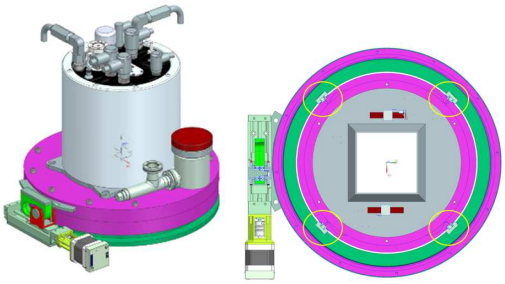

Figure 2: Focusing mechanism at camera level

A 36 Mpixels, 15 µm CCD is a possible option to replace the actual 16 Mpixel sensor. This new sensor presents the very same characteristics as for NEOSTED, only with increased imaging area.

The new Aspherical Lens Support is completely redesigned to be as light as possible and to avoid the obscuration and the interference with the beams of the 8 channels passing through it. It will be evaluated the possibility to realize the new beam splitter as constituted by three monolithic prisms.

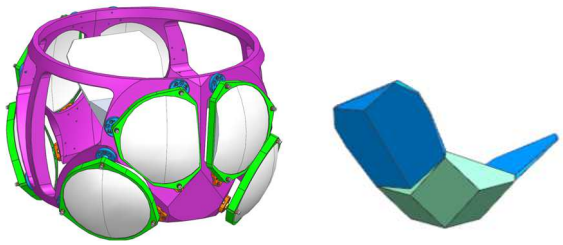

Figure 3: Preliminary Aspherical Lenses Support and Beam Splitter

Due to the experience gained during the activities carried out on first Flyeye, it has been judged useful to implement a new mechanism for the aspherical lens position adjusting and alignment.

The mechanism is constituted by three stations able to realize:

- the lens translation on the plane (±2 mm)
- the lens tip-tilt (about ±0.5° ÷ 0.75°)
- the lens piston (±2 mm)

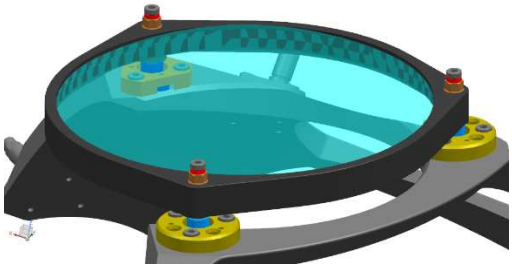

Figure 4: Aspherical Lens Adjustment Mechanism

The SOT has been redesigned with respect to first Flyeye one and it has been optimized for reaching a channel FoV of 3.75 square degrees, while the original Flyeye SOT had a 2.76 square degrees FoV per channel. This improvement provides the newer 8 channels telescope an overall FoV of 30 square degrees, i.e. 40% more than what would have been the original Flyeye design with 8 channel only (22 square degrees).

The final telescope more relevant optical specifications are listed below.

Entrance pupil = 1100 [mm]

Focal length = 2650 [mm]

Central Obstruction = 540 [mm]

Number of optical channels = 8

Field of View = 30 [sq grad]

Primary mirror diameter = 1460 [mm]

F/number = 2,4

7. REDUCED CHANNELS TELESCOPE PERFORMANCES

In the following figures the performances of the telescope will be presented, to be evaluated with respect to the project requirements. The FoV coverage is the percentage of the telescope entire FoV which detects the limit V-mag of 21. The limiting magnitude map illustrates the distribution of the maximum V-band magnitude detectable along the entire telescope FoV.

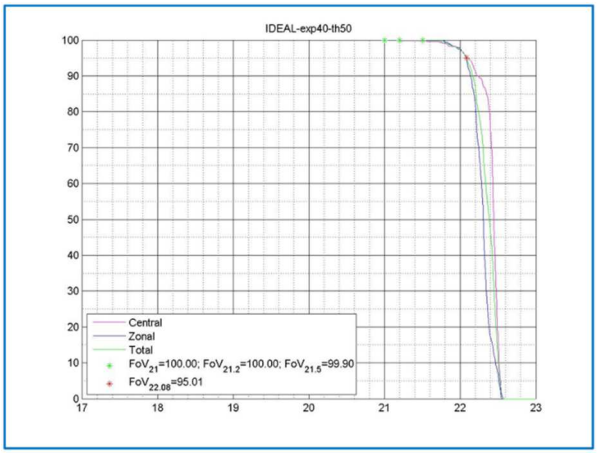

Figure 5: Field of view coverage versus limiting magnitude for the ideal telescope configuration

In the above Figure 5 the FoV coverage versus limiting magnitude is reported, at SNR = 5, for the ideal telescope configuration, seeing = 0 arcsec and not tolerated layout as well, 40 s exposure time.

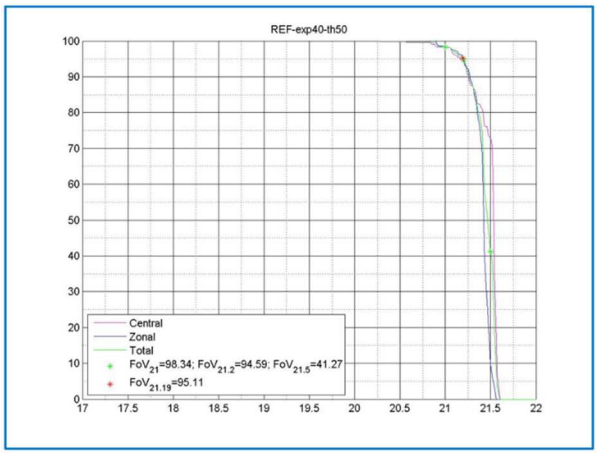

Figure 6: Field of view coverage versus limiting magnitude for the reference telescope configuration

In the above Figure 6 the FoV coverage versus limiting magnitude is reported, at SNR = 5, for the reference telescope configuration, seeing = 1.5 arcsec and not tolerated layout as well, for 40 s exposure time.

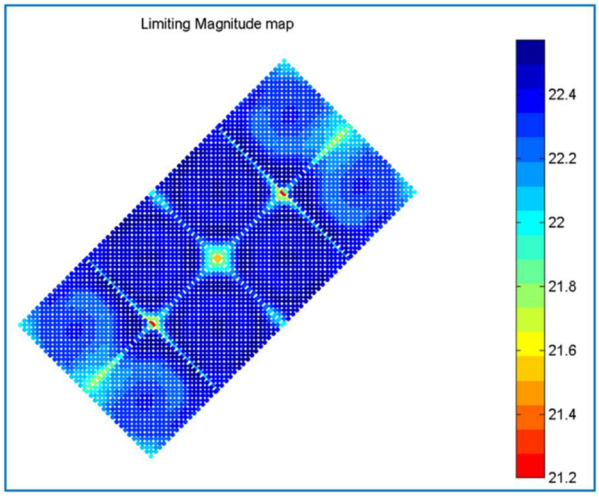

Figure 7: Limiting magnitude distribution along the telescope FoV for the ideal telescope configuration

In the above Figure 7 the limiting magnitude distribution along the telescope FoV is reported, at SNR = 5 for the ideal telescope configuration, seeing = 0 arcsec and not tolerated layout as well, 40 s exposure time.

It can be seen, by a comparison between the above ideal channel limit magnitude map, and the below reference channel one, that the effect of the 1.5 arcsec seeing is to lower the performance of the telescope.

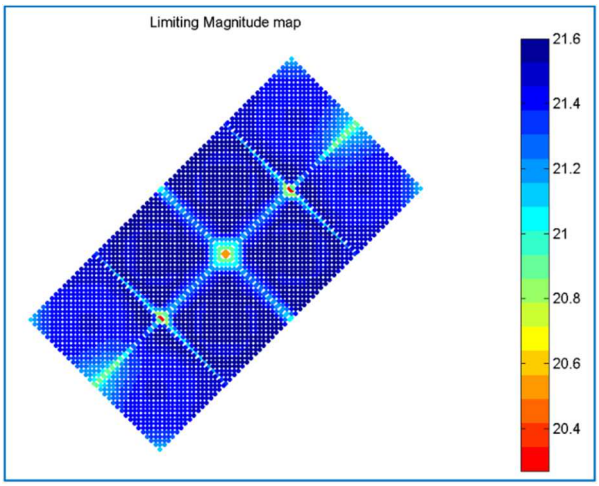

Figure 8: Limiting Magnitude distribution along the telescope FoV for the reference telescope configuration

In the above Figure 8 the limiting magnitude distribution along the telescope FoV is reported, at SNR = 5 for the reference telescope configuration, seeing = 1.5 arcsec and not tolerated layout as well, for 40 s exposure time.

8. SOT MODULARITY AND TELESCOPE SCALABILITY

The newer SOT design has been developed to be applied to different channels configuration telescopes too, i.e.:

- 4 channels - 15 sq. deg. FoV – 4/4 = 1 transitions/ch.
- 8 channels - 30 sq. deg. FoV – 10/8 = 1.25 transitions/ch.
- 12 channels - 45 sqdeg FoV – 17/12 = 1.42 transitions/ch.
- 16 channels - 60 sq. deg. FoV – 24/16 = 1.5 transitions/ch.

At the time of writing, the first 2 configurations have been properly assessed to be fully compliant against the FoV coverage of V-mag 21 requirement. The 12 channels/45 sq. deg. configuration is very promising to be compliant, and also for the 16 channels/60 sq. deg. design the expectations are high. It must be stated that by increasing the overall telescope FoV to the huge value of 60 sq. deg., the difficulties to comply the requirement C will increase. Despite this, the preliminary simulation outcomes currently available show a very high adaptability of the modular design to any expansion of the number of optical channels.

The most important advance of the modular Flyeye is the FoV to telescope envelope ratio. The modular concept allows to compound a huge FoV into a relatively compact unique instrument, in the dimensional range of any modern 1 meter optical telescope.

9. CONCLUSIONS

The modular 8 channels Flyeye telescope can be considered the newer benchmark for monitoring the celestial vault by a fast reconnaissance. It fulfils the driving requirement of detecting asteroids down to V-band magnitude of 21.0 with a minimum peak SNR of 5.0 over at least the 95% of the entire FoV. The modular design allows an easy scaling of the FoV until a predictable value of 60 square degrees, saving an overall telescope envelope in the range of any modern 1 meter optical telescope. Thanks to the Flyeye concept, the envelope limitation of the traditional Schmidt camera, and even of any array of telescopes with the same FoV, are definitely overcome.

10. REFERENCES

1. Cibin, L., Chiarini, M., Gregori, P., Bernardi, F., Ragazzoni, R., Sessler, G., Kugel, U., (2019). The Fly-Eye Telescope, Development and First Factory Tests Results. In Proc. - 1st NEO and Debris Detection Conference, Darmstadt, Germany.
2. Vellutini, E., Gregori, P., Pellegrini, R., Dimare, L., Bernardi, F., Di Cecco, A., Castronuovo, M.M., Marzo, C., Perozzi, E., (2022). Exploiting the synergies of observing NEO and space debris with the Flyeye telescope. 73rd International Astronautical Congress (IAC), Paris, France.
3. Di Cecco, A. et al., Analysis of Italian sites for NEO and space debris observations with the ESA Flyeye telescope, Proc. of the ESA NEO and Debris detection Conference exploiting synergies, 22-14 January 2019, Darmstadt, Germania, published by ESA Space Debris Office;
4. Dotto and the NEOROCKS Team. The EU NEO Rapid Observation, Characterization and Key Simulations project. EPSC Abstracts Vol.15 EPSC2021-389, 2021;